Site-Directed Mutagenesis of the CPa-1 Protein of Photosystem II: Alteration of the Basic Residue Pair ^{384,385}R to ^{384,385}G Leads to a Defect Associated with the Oxygen-Evolving Complex†

Cindy Putnam-Evans and Terry M. Bricker*

Department of Botany, Louisiana State University, Baton Rouge, Louisiana 70803

Received June 8, 1992; Revised Manuscript Received September 16, 1992

ABSTRACT: The *psb*B gene encodes the intrinsic chlorophyll-a binding protein CPa-1 (CP-47), a component of photosystem II in higher plants, algae, and cyanobacteria. Oligonucleotide-directed mutagenesis was used to introduce mutations into a segment of the *psb*B gene encoding the large extrinsic loop region of CPa-1 in the cyanobacterium *Synechocystis* sp. PCC 6803. Altered *psb*B genes were introduced into a mutant recipient strain (DEL-1) of *Synechocystis* in which the genomic *psb*B gene had been partially deleted. Initial target sites for mutagenesis were absolutely conserved basic residue pairs occurring within the large extrinsic loop. One mutation, RR384385GG, produced a strain with impaired photosystem II activity. This strain exhibited growth characteristics comparable to controls. However, at saturating light intensities this mutant strain evolved oxygen at only 50% of the rate of the control strains. Quantum yield measurements at low light intensities indicated that the mutant had 30% fewer fully functional photosystem II centers than do control strains of *Synechocystis*. Immunological analysis of a number of photosystem II protein components indicated that the mutant accumulates normal quantities of photosystem II proteins and that the ratio of photosystem II to photosystem I proteins is comparable to that found in control strains. Upon exposure to high light intensities the mutant cells exhibited a markedly increased susceptibility to photoinactivation. However, Tris-treated thylakoid membranes from both the mutant and wild-type exhibited comparable rates of photoinactivation. Thylakoid membranes isolated from RR384385GG exhibited only 15% of the H_2O to 2,6-dichlorophenolindophenol electron transport rate observed in wild-type strains. The 1,5-diphenylcarbazide to 2,6-dichlorophenolindophenol electron transport rates of Tris-treated thylakoids from the mutant, however, were comparable to control rates. These results suggest that alteration of this basic residue pair leads to a defect associated with the oxygen-evolving complex of photosystem II.

Photosystem II (PS II)[1] is a multisubunit thylakoid membrane protein complex which catalyzes the light-driven oxidation of water to molecular oxygen and the reduction of plastoquinone to plastoquinol. This complex consists of both intrinsic and extrinsic protein subunits. Intrinsic polypeptides with apparent molecular masses of 49 (CPa-1), 45 (CPa-2), 34 (D1), 32 (D2), 9 and 4.5 (α and β subunits of cytochrome b_{559}), and 4 kDa (*psb*I gene product) appear to form the minimum complex capable of photosynthetic oxygen evolution (Burnap & Sherman, 1991; Philbrick et al., 1991; Bricker, 1992). Extrinsic proteins with apparent molecular masses of 33 (manganese-stabilizing protein), 24, and 17 kDa are required for optimal oxygen evolution rates at in vivo concentrations of calcium and chloride in higher plants and green algae; the cyanobacteria lack the 24- and 17-kDa components. A number of other low molecular weight proteins have been identified which seem to be associated with PS II; however, their functions have not been clearly defined (Ikeuchi et al., 1989). Oxygen evolution also requires the presence of four manganese, one or two calcium, and several chloride ions (Amesz, 1983; Dismukes, 1986; Homann, 1987). The binding sites for these cofactors remain largely undetermined.

CPa-1 (CP-47), a component of the interior antenna of PS II, is an integral membrane protein which is predicted to contain six membrane-spanning α-helical domains (Vermaas et al., 1987; Bricker, 1990). This protein contains a large lumenally exposed hydrophilic loop which spans amino acid residues ^{257}W–^{450}W (Bricker, 1990) and is located between the fifth and sixth transmembrane helixes. One function of CPa-1 is the transfer of excitation energy from the light-harvesting pigment proteins to the reaction center of the photosystem. Additionally, all oxygen-evolving preparations isolated to date contain this protein (Ghanotakis et al., 1987; Tang & Satoh, 1985). We have demonstrated that CPa-1 is closely associated with components required for oxygen evolution. A monoclonal antibody has been produced which recognizes its antigenic determinant within the large extrinsic loop of CPa-1 only after the chloride-insensitive pool of manganese associated with the oxygen-evolving complex has been removed from PS II membranes (Bricker & Frankel, 1987; Frankel & Bricker, 1989). CPa-1 is also closely associated with the manganese-stabilizing protein. CPa-1 is shielded from tryptic attack by the manganese-stabilizing protein (Bricker & Frankel, 1987). Lysyl residues located in the large extrinsic loop of CPa-1 are labeled with NHS-biotin only in the absence of the manganese-stabilizing protein (Bricker, et al., 1988; Frankel & Bricker, 1992). Cross-linking of CPa-1 and the manganese-stabilizing protein with a zero-length cross-linker EDC (Bricker et al., 1988; Enami et al., 1991) suggests that these proteins interact via a salt bridge.

† This work was sponsored by USDA–NRICGP Grant 91-37036-6350 to T.M.B.

[1] Abbreviations: bp, base pairs; chl, chlorophyll; DCBQ, 2,6-dichloro-*p*-benzoquinone; DCPIP, 2,6-dichlorophenolindophenol; DPC, 1,5-diphenylcarbazide; DTSP, dithiobis(succinimidyl propionate); EDC, 1-ethyl-3-[3-(dimethylamino)propyl]carbodiimide; HEPES, *N*-(2-hydroxyethyl)-piperazine-*N*′-2-ethanesulfonic acid; kb, kilobase; MES, 2-(*N*-morpholino)-ethanesulfonic acid; NHS-biotin, *N*-hydroxysuccinimidobiotin; PCR, polymerase chain reaction; PS I, photosystem I; PS II, photosystem II; TES, *N*-[tris(hydroxymethyl)methyl]-2-aminoethanesulfonic acid; Tris, tris(hydroxymethyl)aminomethane.

0006-2960/92/0431-11482$03.00/0

Cross-linking of these two proteins with other reagents has also been observed (Enami et al., 1987; Bricker et al., 1988; E. Camm, personal communication).

CPa-1 is encoded by the *psb*B gene, which is located in the chloroplast genome of green algae and higher plants and the nuclear genome of cyanobacteria. Insertional mutagenesis (Vermaas et al., 1987) or deletion (Eaton-Rye & Vermaas, 1991a) of the *psb*B gene leads to a PS II$^-$ phenotype, and it has been hypothesized that CPa-1 is required for PS II assembly (Vermaas et al., 1988). Only a few site-directed mutants have been produced in CPa-1. Eaton-Rye and Vermaas (1991b) have produced a number of mutations in the conserved histidines which are located near the membrane surface in transmembrane helixes II and VI. One of these, H466Q, grows slower than does wild-type, has a 5-fold higher chl/PS II ratio, and exhibits a greatly reduced 695-nm 77 K fluorescence emission peak. These authors concluded that ^{466}H is required for the stable incorporation of CPa-1 into the photosynthetic membrane. Two deletion mutants have been produced in the large extrinsic loop (Eaton-Rye & Vermaas, 1991a). One of these, Δ(G351–T365), exhibits a PS II$^-$ phenotype and does not appear to contain assembled PS II centers although it does accumulate immunologically detectable quantities of CPa-1, CPa-2, D1, and D2. The other deletion mutant, Δ(R384–V392), assembles functional PS II centers, although in smaller numbers than is observed in wild-type, and exhibits steady-state oxygen evolution rates which are about 50% of those observed in wild-type.

The large extrinsic loop of CPa-1 contains a large number of conserved amino acid residues (Bricker, 1990). An unusual feature of the loop is the presence of four basic residue *pairs*. It has been suggested that these residues might provide sites for manganese ligation via chloride bridging ligands (Morris & Herrmann, 1984). It is also possible that some of the basic residues in the large extrinsic loop provide sites for interaction of CPa-1 with the manganese-stabilizing protein or other extrinsic or intrinsic proteins of the PS II complex or ionic cofactors. We have chosen these sites for mutagenesis in order to determine the potential roles of these amino acids in CPa-1 function. In this paper, we report that alteration of the basic residue pair ^{384,385}R to ^{384,385}G leads to a marked loss of PS II activity which is associated with a defect at the oxygen-evolving complex of PS II.

MATERIALS AND METHODS

Growth Conditions. Wild-type and mutant *Synechocystis* sp. PCC 6803 were grown in liquid BG-11 media (Rippka, 1979) at room temperature and at light intensities of 20 μmol of photons·(m^2)$^{-1}$·s^{-1} on a rotary shaker. The *psb*B partial deletion strain (Del-1) was grown in BG-11 media containing 5 mM glucose. Cultures on plates were maintained in BG-11 supplemented with 1.5% agar, 0.3% sodium thiosulfate, 10 mM TES–KOH, pH 8.2, and 5 mM glucose (where appropriate). For the preparation of thylakoid membranes, control and mutant cells were grown in 15-L carboys in BG-11 media supplemented with 0.3% sodium thiosulfate, 5 mM glucose, 10 mM TES–NaOH, pH 8.2, and appropriate antibiotics. Antibiotics were added to the media at a final concentration of 10 μg/mL.

Site-Directed Mutagenesis. Restriction digests, cloning, growth and transformation of bacterial strains, and isolation of DNA fragments were performed according to standard procedures (Maniatis et al., 1982). Phagemid isolations were performed using disposable anion-exchange columns (Qiagen Inc.).

A 1.4-kb *Kpn*I/*Kpn*I fragment of *psb*B (kindly provided by Dr. Wim Vermaas) encoding the C-terminal portion of CPa-1 was cloned into the multiple cloning site of the phagemid pTZ18U (BioRad). This fragment contains the coding region for the entire large extrinsic loop of CP-47 as well as 0.7 kb of the 3′ flanking sequence. A 1.2-kb kanamycin resistance gene was excised from the plasmid pUC-4K and inserted into an *Nco*I site 369 base pairs downstream of the *psb*B coding sequence to produce the phagemid pTZ18K3. Transformation of wild-type *Synechocystis* with pTZ18K3 which contained no site-directed modifications yielded the control *Synechocystis* strain K3. This strain contains an intact *psb*B gene with a kanamycin resistance cartridge located 369 base pairs from the 3′ end of the *psb*B gene. Desired mutations were introduced into pTZ18K3 by oligonucleotide-directed mutagenesis using the procedure of Kunkel et al. (1985). Synthetic oligonucleotides were constructed to give the requisite arginyl to glycyl changes (see Results). Mutant phagemids were sequenced (Sequenase, USB) in order to confirm the presence of the appropriate mutations prior to transformation into the spectinomycin-resistant *psb*B partial deletion strain (see below). Transformations were carried out by the procedure of Williams (1988). Colonies of putative site-directed mutants were screened for kanamycin resistance and spectinomycin sensitivity. Colonies were also streaked on kanamycin-containing plates in the presence or absence of glucose, to screen for the possible loss of photoautotrophic growth.

Construction of a psbB Partial Deletion Strain. A strain of *Synechocystis* 6803 exhibiting a PS II$^-$ phenotype (designated DEL-1) was produced in order to serve as the recipient strain for the mutant (site-directed) phagemids. A phagemid was constructed by replacing the 1 kb *Bst*EII/*Nco*I fragment (encoding 55% of the large extrinsic loop as well as the kanamycin resistance gene) of pTZ18K3 with a 2.0-kb spectinomycin resistance gene excised from pBR322-Ω. This resulting phagemid was used to transform wild-type *Synechocystis* 6803. Colonies were selected for photoheterotrophic growth on plates containing glucose and spectinomycin.

PCR and DNA Sequencing. To confirm the mutations, genomic DNA was isolated from putative mutants from cell lysates according to the procedure of Williams (1988) except that the cesium chloride ultracentrifugation steps were omitted. Oligonucleotides flanking the *Kpn*I/*Kpn*I fragment of the *psb*B gene were used to amplify this region from the genomic DNA of each mutant using the polymerase chain reaction. The thermal cycling routine consisted of the following steps performed on 100-μL reactions: 1-min denaturation at 93 °C, 45-s annealing at 65 °C, and 2-min elongation at 72 °C, for a total of 20 cycles. The PCR products were directly cloned into the plasmid pCR-1000 (InVitrogen), and plasmids were sequenced by the double-stranded Sequenase (USB) method.

Oxygen Evolution Assays. PS II activity was measured by O_2 polarography using a Hansatech oxygen electrode. The cells were assayed in BG-11 media with either 5 mM sodium bicarbonate or 1 mM DCBQ added as an electron acceptor. The light intensity in these experiments was 3000 μmol of photons·(m^2)$^{-1}$·s^{-1} of copper sulfate-filtered white light at 25 °C. For the light saturation experiments, the light intensity was varied between 25 and 4800 μmol of photons·(m^2)$^{-1}$·s^{-1}. Light intensity was measured with a spectroradiometer (Li-Cor, Inc.) equipped with a quantum probe. For the whole-cell photoinactivation experiments, cells were incubated in BG-11 media at a chl concentration of 10 μg/mL at either

2000 or 4000 μmol of photons·$(m^2)^{-1}$·s^{-1} at 25 °C. At various times aliquots were removed, 1 mM DCBQ added, and the samples assayed for oxygen-evolving activity. The chl concentration in all of these oxygen evolution assays was 10 μg/mL. In whole cells, chl was measured by the method of Williams (1988) while in thylakoid membranes chl was measured by the method of Arnon (1949).

Thylakoid membranes were isolated by the method described by van der Bolt and Vermaas (1992) with the exception that the breaking buffer consisted of 50 mM HEPES–NaOH, pH 7.0, 5 mM $MgCl_2$, 5 mM $CaCl_2$, and 1 M sucrose (Yu & Vermaas, 1991). Water to DCPIP measurements were performed at a chl concentration of 10 μg/mL and a DCPIP concentration of 100 μM in a buffer consisting of 300 mM sucrose, 15 mM NaCl, 10 mM $MgCl_2$, 5 mM $CaCl_2$, and 50 mM MES–NaOH, pH 6.0. For the DPC to DCPIP measurements, the thylakoid membranes were first treated with 1 M Tris-HCl, pH 9.2, 300 mM sucrose, 15 mM NaCl, and 10 mM $MgCl_2$ for 1 h and then washed twice with 300 mM sucrose, 15 mM NaCl, 10 mM $MgCl_2$, 5 mM $CaCl_2$, and 50 mM MES–NaOH, pH 6.0. The Tris-extracted membranes were then assayed for PS II activity at a chl concentration of 10 μg/mL, a DCPIP concentration of 100 μM, and a DPC concentration of 500 μM in a buffer consisting of 300 mM sucrose, 15 mM NaCl, 10 mM $MgCl_2$, 5 mM $CaCl_2$, and 50 mM MES–NaOH, pH 6.0. For some experiments 500 μM DPC was added to non-Tris-washed thylakoid membranes. All of these assays were performed at 25 °C at a white light concentration of 3000 μmol of photons·$(m^2)^{-1}$·s^{-1}. For the photoinactivation experiments performed on membranes, Tris-extracted thylakoids were suspended at a chl concentration of 10 μg/mL in 300 mM sucrose, 15 mM NaCl, 10 mM $MgCl_2$, 5 mM $CaCl_2$, and 50 mM MES–NaOH, pH 6.0, and irradiated with white light at 2000 μmol of photons·$(m^2)^{-1}$·s^{-1} at 25 °C. Aliquots were removed at various times, brought to a DCPIP concentration of 100 μM and a DPC concentration of 500 μM, and assayed at 3000 μmol of photons·$(m^2)^{-1}$·s^{-1} at 25 °C. The reduction of DCPIP was measured at 590 nm with a molar extinction coefficient of 16 000 (Allen & Holmes, 1986).

Electrophoresis and Immunological Analysis. Electrophoresis, "Western blotting", and antibody probing were performed as previously described (Bricker et al., 1988). The anti-manganese-stabilizing protein antibody used in this study was produced by immunization of mice with manganese-stabilizing protein purified by the procedure of Kuwabara et al. (1985). This purified protein also cross-reacts with a monoclonal antibody, FCC4, which recognizes the manganese-stabilizing protein (Frankel & Bricker, 1990). The anti-CPa-1 and anti-CPa-2 antibodies used were gifts from Dr. N.-H. Chua and were originally raised against the purified peptides "5" and "6" from *Chlamydomonas* (Chua & Bloomberg, 1979). Anti-CP I was provided by Dr. J. Guikema and was raised against synthetic peptides with sequences corresponding to C-terminal *Anacystis nidulans* R2 *psa*B sequences (R. Henry and J. A. Guikema, personal communication). The anti-D1 antibody was supplied by Dr. A. Trebst and was produced by immunization with a β-galactosidase–*psb*A fusion protein.

RESULTS AND DISCUSSION

A partial restriction map of the *psb*B gene which encodes CPa-1 is shown in Figure 1A. The parental plasmid used for mutagenesis (pTZ18K3) consisted of the *Kpn*I/*Kpn*I fragment of this gene cloned into the *Kpn*I site of the phagemid pTZ18U.

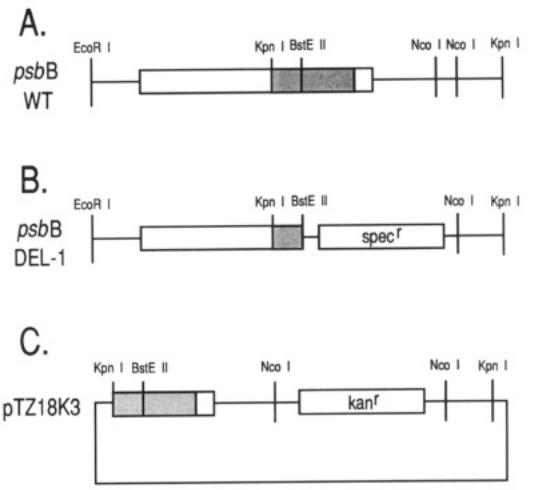

FIGURE 1: Partial restriction maps of (A) the genomic *psb*B gene; (B) the genomic *psb*B gene of the recipient deletion strain, DEL-1; and (C) the phagemid pTZ18K3. Regions which encode portions of the large extrinsic loop are shaded.

To aid in screening and maintenance of potential mutant phenotypes, a kanamycin resistance gene was inserted at the *Nco*I site located 369 base pairs downstream of the *psb*B coding sequence (Figure 1C). Wild-type *Synechocystis* was transformed with nonmutagenized pTZ18K3 in order to produce the control strain K3. This strain is identical to wild-type with the exception that K3 contains the kanamycin resistance gene downstream from the *psb*B gene.

Construction of DEL-1. In order to facilitate the screening for putative mutants, a partial deletion strain of *Synechocystis* (designated DEL-1) was constructed to serve as the recipient strain for pTZ18K3 plasmids bearing the desired mutations. pTZ18K3 was cut with *Bst*E and *Nco*I in order to remove nucleotides 1392–2385 from the *Kpn*I/*Kpn*I fragment of the *psb*B gene. This region was replaced with a gene conferring spectinomycin resistance (Figure 1B). The part of *psb*B encoded in the *Bst*EII/*Nco*I fragment included the target area for mutagenesis in addition to 0.32 kb of 3′ flanking DNA and the kanamycin resistance marker. Importantly, the plasmid used to construct DEL-1 contains approximately 250 base pairs of *psb*B sequence 5′ to the *Bst*EII site and 200 base pairs of *psb*B 3′ flanking sequence downstream of the kanamycin cartridge. This flanking sequence is absolutely required for the incorporation (by homologous recombination) of altered *psb*B at the genomic *psb*B site. Following transformation of wild-type 6803, spectinomycin-resistant, kanamycin-sensitive colonies were recovered. Genomic *psb*B DNA from DEL-1 was PCR amplified, cloned, and sequenced as described in the Materials and Methods. Sequencing of the amplified DNA confirmed that nucleotides 1392–2385 had been deleted in the DEL-1 strain (data not shown). The DEL-1 mutant is an obligate photoheterotroph (data not shown).

Alteration of the Basic Residue Pair ^{384,385}R to ^{384,385}G in CPa-1. As discussed previously, we chose conserved basic residues residing within the large extrinsic loop of CPa-1 as initial sites for site-directed mutagenesis. For the mutant described in this paper (RR384385GG), a mutagenic oligonucleotide with the sequence 5′-GGGCGGATATTCCCT-TCGGTGGTTCCGAGTCTAAATTCAGTCT-3′ was used to convert a pair of arginine residues at positions 384 and 385 in the amino acid sequence of CPa-1 to a pair of glycine residues. The left panel of Figure 2 shows the genomic DNA sequence from wild-type 6803 from nucleotides 1500–1529. The two arginine codons are indicated. The right panel shows

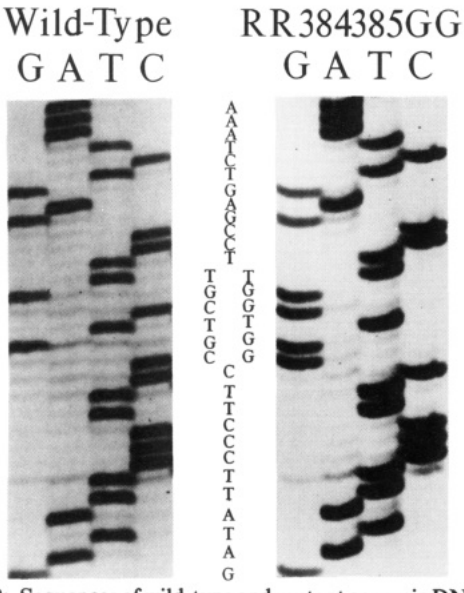

FIGURE 2: Sequences of wild-type and mutant genomic DNAs. PCR was used to amplify the *Kpn*I/*Kpn*I fragment of the *psb*B gene from genomic DNA isolated from the site-directed mutant and the wild-type. The wild-type sequence is shown to the left, and the RR384385GG sequence is shown to the right. The nucleotide sequences of wild-type and the mutant are shown down the center of the panel.

the genomic DNA sequence of the RR384385GG mutant, at the same nucleotide positions as shown for wild-type. The two arginine codons (CGT) were changed to GGT, which encodes glycine, thus demonstrating that RR384385GG is the intended mutant.

Characterization of RR384385GG. Growth studies indicated that wild-type, K3, and the RR384385GG mutant strain all exhibited comparable rates of photoautotrophic growth in liquid culture. DEL-1, which lacks part of its *psb*B coding sequence, did not grow photoautotrophically in the absence of glucose (data not shown).

Photosynthetic electron transport activities in the various strains are shown in Table I. There was no significant difference between wild-type and K3 photosynthetic electron transport rates in either whole cells or thylakoids (data not shown). DEL-1 cells exhibited no detectable oxygen evolution using either CO_2 or DCBQ as an electron acceptor. In whole cells, the measurement of whole-chain electron transport from H_2O to CO_2 demonstrated that oxygen evolution rates of RR384385GG were 40% of that observed for K3. The PS II-dependent oxygen evolution activity (H_2O to DCBQ) for the mutant RR384385GG was about 50% of the rate observed for K3. These results indicate that the lesion associated with the introduction of this site-directed mutation into CPa-1 resides in PS II, as was expected.

Figure 3 illustrates the results obtained from the immunological analysis of a number of PS II components (CPa-1, CPa-2, D1, and the manganese-stabilizing protein) and one of the two P-700 chl-a binding polypeptides of photosystem I (*psa*B gene product), CP I. It is apparent that very similar quantities of all of these components are present in K3 and RR384385GG. Similar results were obtained for the deletion mutant Δ(R384–V392) in CPa-1 (Eaton-Rye & Vermaas, 1991a). It should be noted that these data are qualitative in nature and that no quantitative interpretations are warranted. It is unlikely, in this experiment, that we would have been able to detect less than a 20–30% difference in the amounts of the various antigens.

Measurement of PS II-dependent (H_2O to DCBQ) oxygen evolution rates of K3 and the RR384385GG cells at light intensities ranging from 150 to 4800 μmol of photons·$(m^2)^{-1}$·s^{-1} produced the light saturation curves shown in Figure 4A. The V_{max} observed in the RR384385GG was 200 μmol of O_2·(mg of chl)$^{-1}$·h^{-1}, 50% of the rate observed for the control strain K3. Figure 4B shows the result of quantum yield experiments, measuring H_2O to DCBQ electron transport activities, performed with K3 and RR384385GG cells. At low light intensities, examination of the first-order rate constants allows the estimation of the relative quantum yield exhibited by these two cyanobacterial strains. RR384385GG exhibited a quantum yield of 0.7 with respect to K3. A number of interpretations are consistent with these results. First, RR384385GG may have, on a chl basis, 30% fewer PS II centers than does K3. Second, RR384385GG may have the same number of PS II centers as K3, but 30% of the PS II centers are inactive. In either of these instances, the centers which are active must evolve oxygen at about 70% of the maximum rate observed in control PS II centers to yield the observed V_{max}, which is 50% of the control oxygen evolution rate. In other words, factors other than the number of active PS II centers may limit V_{max} in RR384385GG. It is likely that at saturating light intensities significant photoinactivation occurs during the course of the oxygen evolution assays (see Figure 5 and Discussion). This would limit the observed V_{max} of the mutant much more so than that of K3. If equivalent numbers of functional PS II centers are present in K3 and RR384385GG, the lower quantum yield could be the result of the presence in RR384385GG of PS II centers which are less efficient in carrying out stable charge separation. If, for instance, the introduction of the site-directed mutation in RR384385GG led to a substantially increased probability of charge recombination within the PS II reaction center and the oxygen-evolving complex, a lower quantum yield would be observed. It should be noted that the DPC to DCPIP electron transport rates of thylakoids isolated from K3 and RR384385GG suggest that these two strains contain similar numbers of active PS II centers (Table I).

Figure 5 demonstrates that the PS II activity, measuring H_2O to DCBQ electron transport activities, of RR384385GG cells was more susceptible to photoinactivating radiation than that of K3 cells. At 2000 μmol of photons·$(m^2)^{-1}$·s^{-1} of white light the $T_{1/2}$ for photoinactivation is 12 min for K3 and 6 min for RR384385GG (Figure 5A) while at 4000 μmol of photons·$(m^2)^{-1}$·s^{-1} of white light the $T_{1/2}$ for photoinactivation is 6 min for K3 and 3 min for RR384385GG (Figure 5B). It should be pointed out that it is very unlikely that the increased photoinactivation rate observed in RR384385GG could be due to the mutation affecting the antennae functions of this protein. Mutations which affect excitation energy transfer from the antennae to the reaction center would be expected to result in decreased rates of photoinactivation, not the increased rates which were observed for RR384385GG. The increased susceptibility of RR384385GG to photoinactivation is comparable in magnitude to that observed in the E69Q and P161L mutants in the D2 protein of *Synechocystis* (van der Bolt & Vermaas, 1992). The E69Q mutation is believed to affect the stability and/or ligation of the manganese cluster while the P161L mutation is located near Y_D and is believed to affect the efficiency of transfer of electrons from the oxygen-evolving site to Y_z^+. These authors hypothesize that decreased rates of electron transfer from the oxygen-evolving complex to Y_z^+, which was observed in both of these mutants, resulted

Table I: Electron Transport Activities of Whole Cells and Thylakoid Membranes[a]

	whole cells		thylakoid membranes			
cell type	$H_2O \rightarrow CO_2$ [μmol of O_2·(mg of chl)$^{-1}$·h^{-1}]	$H_2O \rightarrow$ DCBQ [μmol of O_2·(mg of chl)$^{-1}$·h^{-1}]	$H_2O \rightarrow$ DCBQ [μmol of O_2·(mg of chl)$^{-1}$·h^{-1}]	$H_2O \rightarrow$ DCPIP [μequiv·(mg of chl)$^{-1}$·h^{-1}]	DPC[b] $\rightarrow$ DCPIP [μequiv·(mg of chl)$^{-1}$·h^{-1}]	H_2O[c] + DPC $\rightarrow$ DCPIP [μequiv·(mg of chl)$^{-1}$·h^{-1}]
K3	156 ± 18[d] (100)[e]	428 ± 89 (100)	163 ± 35 (100)	144 ± 24 (100)	165 ± 17 (100)	201 ± 37 (100)
RR384385GG	63 ± 23 (40)	224 ± 69 (52)	49 ± 2 (30)	22 ± 14 (15)	146 ± 5 (88)	111 ± 5 (55)
DEL-1	0 (0)	0 (0)	ND[f]	ND	ND	ND

[a] All rates shown are the average of at least three independent experiments. [b] Tris-washed membranes. [c] Membranes not tris-washed. [d] 1.0 standard deviation. [e] % of K3 rate. [f] Not determined.

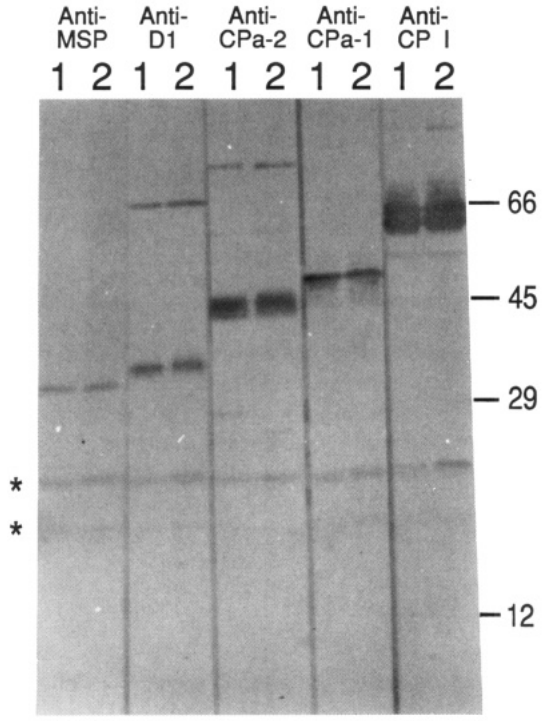

FIGURE 3: "Western blots" of K3 and RR384385GG membrane proteins. Thylakoid membranes were isolated as described in Materials and Methods. Three micrograms of chl of K3 and RR384385GG membranes were separated by LDS–PAGE (12.5–20% acrylamide gradient), electroblotted onto PVDF membranes, and, after blocking and washing, probed with various primary antibodies. The protein bands were visualized by incubation with the appropriate peroxidase-conjugated secondary antibody and color development with 4-chloro-1-naphthol + H_2O_2. Lane 1, K3 membrane proteins; lane 2, RR384385GG membrane proteins. The primary antibody is indicated above. Apparent molecular masses are shown on the right. Asterisks indicate blue phycobiliproteins.

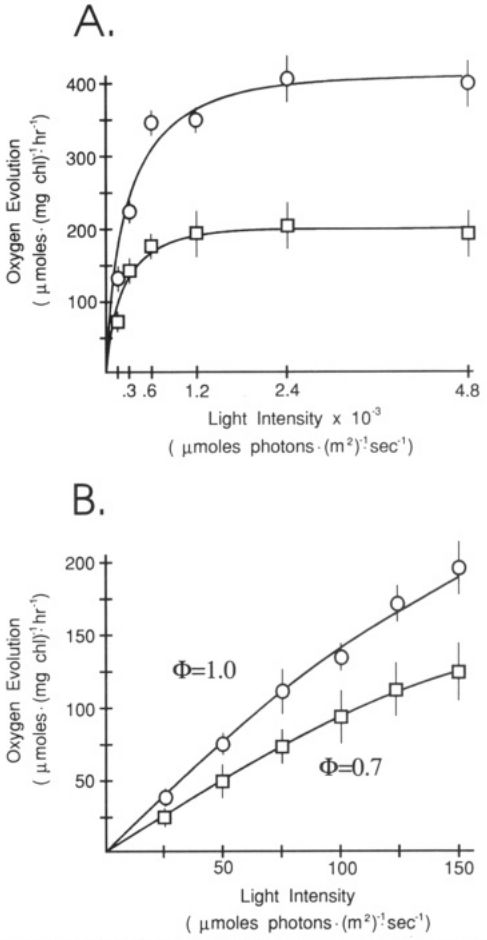

FIGURE 4: (A) PS II (H_2O to DCBQ) light saturation curves for K3 and the mutant RR384385GG cells are shown. The V_{max} for RR384385GG is about 50% of that observed for K3. (B) The results of quantum yield experiments for K3 and the mutant RR384385GG cells are shown. Analysis of the first-order rate constants for K3 and RR384385GG suggests that there are approximately 30% fewer active PS II centers in the mutant than in the wild-type. The relative quantum yields are shown. These data are the result of two experiments. Error bars = 1 standard deviation. Open circles, K3; open squares, RR384385GG.

in the accumulation of oxidizing side radicals (such as Y_z^+ and P_{680}^+) which damage the PS II reaction center and lead to the observed photoinactivation. Since numerous lines of evidence exist which suggest that CPa-1 closely interacts with the oxygen-evolving complex (see below), we hypothesize that a similar mechanism may be occurring in RR384385GG.

An experiment which supports this hypothesis is shown in Figure 6. Photoinactivation experiments performed on Tris-washed thylakoid membranes indicate that the RR384385GG does not photoinactivate more rapidly than does the control strain K3. In these experiments the oxygen-evolving complex has been removed by Tris-washing. The absence of an enhanced rate of photoinactivation for Tris-washed RR384385GG membranes suggests that the differential photoinactivation observed in whole cells is due to a lesion in the oxygen-evolving complex of PS II and may suggest that aberrant rates of electron transfer from the oxygen-evolving complex to Y_z may be occurring in RR384385GG, as was observed in the E69Q and P161L of the D2 protein (van der Bolt & Vermaas, 1992).

To further examine the nature of the functional lesion induced in this mutant, thylakoid membranes were isolated from both K3 and RR384385GG. Table I summarizes the results obtained from examining the PS II electron transport rates observed in these membranes. The mutant RR384385GG exhibits a marked reduction in H_2O to DCBQ and H_2O to DCPIP electron transport capability (30% and 15%, respectively) when compared with K3. This result is consistent with the results obtained in whole cells, although of larger magnitude (see below). The measurement of DPC to DCPIP electron transport rates in Tris-washed membranes,

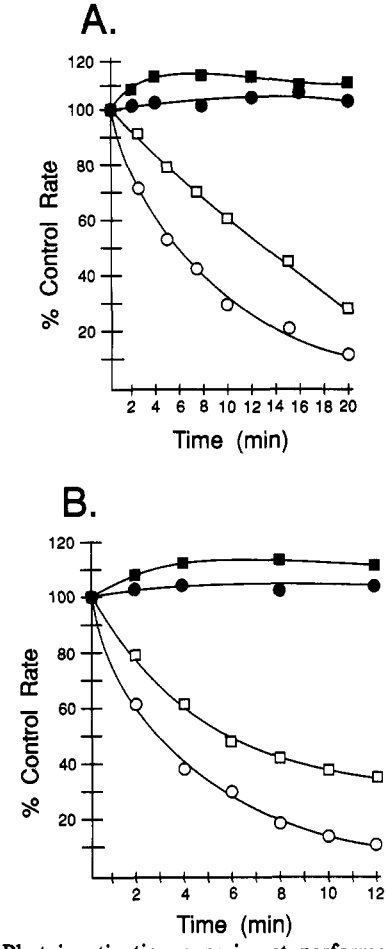

FIGURE 5: Photoinactivation experiment performed on K3 and RR384385GG cells at (A) 2000 μmol of photons·$(m^2)^{-1}$·s^{-1} and (B) 4000 μmol of photons·$(m^2)^{-1}$·s^{-1}. Note different time axes in panels A and B. Closed squares, K3 cells, no photoinactivating light; closed circles, RR384385GG cells, no photoinactivating light; open squares, K3 cells plus photoinactivating light; open circles, RR384385GG cells plus photoinactivating light. The data shown are the average of three experiments. The standard deviations for these data points average 5.1%. The 100% rates for K3 and RR384385GG are as shown in Table I.

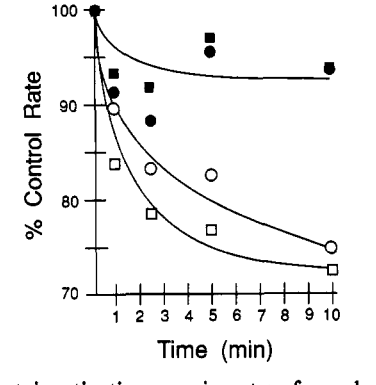

FIGURE 6: Photoinactivation experiment performed on Tris-washed K3 and RR384385GG thylakoid membranes at 2000 μmol of photons·$(m^2)^{-1}$·s^{-1}. Closed squares, K3 cells, no photoinactivating light; closed circles, RR384385GG cells, no photoinactivating light; open squares, K3 cells plus photoinactivating light; open circles, RR384385GG cells plus photoinactivating light. The data shown are the average of three experiments. The standard deviations for these data points average 7.5%. The 100% rates for K3 and RR384385GG are as shown in Table I.

however, indicated that there was no significant difference between the mutant RR384385GG and K3. Since DPC donates electrons to PS II at the level of Y_z, these results clearly demonstrate that the electron transport defect observed in RR384385GG thylakoids is associated with the oxygen-evolving complex of PS II. This result also suggests that, on a chl basis, K3 and RR384385GG contain similar numbers of active PS II centers.

The low rate of water-dependent electron transport observed in the thylakoid membranes of RR384385GG suggests that the oxygen-evolving complex of this mutant is much more labile during thylakoid isolation than are the complexes from K3 membranes. In Table I, the electron transport rates of non-Tris-washed thylakoids which have been supplemented with DPC are shown. DPC is a poor electron donor to PS II in the presence of an intact oxygen-evolving complex. K3 membranes exhibit a 1.4-fold stimulation in DCPIP reduction upon the addition of DPC while RR384385GG membranes exhibit a 5-fold stimulation in activity. These data suggest that, during thylakoid membrane isolation from RR384385GG, the majority of PS II centers exhibit damage to their oxygen-evolving complexes, allowing enhanced donation of electrons from DPC. These findings clearly demonstrate that alteration of this basic residue pair (^{384,385}R to ^{384,385}G) dramatically affects the in vitro stability of the oxygen-evolving complex of PS II.

It is interesting to compare the results we have obtained for RR384385GG and the results obtained for Δ(R384–V392) by Eaton-Rye and Vermaas (1991a) since our site-directed alteration lies within their deletion. Both mutants are photoautotrophic, grow at the same rate as do control *Synechocystis* strains, and accumulate near-normal amounts of a number of PS II components. Additionally, in whole cells, both mutants exhibit a V_{max} for oxygen evolution which is about 50% of that observed in the controls. Interestingly, [^{14}C]diuron binding data suggest that Δ(RR384–V392) possesses about 1/3 of the number of PS II centers that are observed in wild-type and that the binding affinity for diuron was not altered. This finding led these workers to suggest that Δ(R384–V392) exhibits a more rapid turnover of PS II centers than does wild-type, although no direct evidence for this speculation was presented. Furthermore, they hypothesized that this lower number of PS II centers could account, at least partially, for the lowered V_{max} for oxygen evolution observed. These authors did not present any findings suggesting that Δ(R384–V392) exhibited a lesion in the oxygen-evolving complex. Our quantum yield measurements on RR384385GG demonstrate that this mutant possesses 30% fewer fully functional PS II centers than are present in controls. Additionally, photoinactivation measurements performed on whole cells and on Tris-washed thylakoids suggest that a defect exists in this mutant which perturbs the transport of electrons from the oxygen-evolving complex to the reaction center of PS II. Furthermore, electron transport measurements on isolated thylakoids of RR384385GG demonstrate that the oxygen-evolving complex of the mutant is very labile and appears to be markedly less stable than that of the control strain. These findings clearly suggest that this site-directed alteration in CPa-1 has damaged the oxygen-evolving complex of PS II.

A number of lines of evidence have suggested that CPa-1 is closely associated with the oxygen-evolving complex of PS II. We have isolated a monoclonal antibody, FAC2, which recognizes its antigenic determinant on CPa-1 only on spinach PS II membranes which have been depleted of the two chloride-insensitive manganese associated with the oxygen-evolving complex (Bricker & Frankel, 1987). The antigenic determinant for this monoclonal antibody has been mapped and is

located within the large extrinsic loop of CPa-1, between ^{360}P and ^{391}S (Frankel & Bricker, 1989). Interestingly, the mutation RR384385GG lies within this epitopic domain.

Additionally, we have found that the manganese-stabilizing protein shields lysyl residues located on CPa-1 from labeling with the amino group-modifying reagent NHS-biotin. Treatments which remove the manganese-stabilizing protein from spinach PS II membranes allow the specific binding of CPa-1 with this reagent. Recently, we have mapped the biotinylated regions on CPa-1 (Frankel & Bricker, 1992). Two domains, ^{304}K–^{321}K and ^{389}K–^{419}K, both of which lie in the large extrinsic loop of CPa-1, are the only biotinylated regions on this protein. It should be noted that the mutant RR384385GG lies in close proximity to the ^{389}K–^{419}K biotinylated domain.

Finally, a variety of protein cross-linkers are capable of cross-linking CPa-1 to the manganese-stabilizing protein in spinach PS II membranes. These include DTSP (Enami et al., 1987; Bricker et al., 1988), 2-iminothiolane (E. Camm, personal communication; C. B. Queirolo, and T. M. Bricker, unpublished observations), and the water-soluble carbodiimide EDC (Bricker et al., 1988; Enami et al., 1991). EDC is particularly interesting since it cross-links amino groups to carboxyl groups which are in van der Waals contact (Hackett & Strittmatter, 1984) and proteins cross-linked by this reagent are assumed to be interacting via a salt bridge. Recently, we have mapped the domains on both the manganese-stabilizing protein and CPa-1 which are cross-linked with EDC. The domain ^{364}E–^{440}D of CPa-1, which is located within the large extrinsic loop, is cross-linked to the N-terminal domain (^{2}E–^{76}K) of the manganese-stabilizing protein (Odom & Bricker, 1992).

CONCLUSIONS

The results presented in this paper strengthen the hypothesis that CPa-1 interacts with the oxygen-evolving site of PS II, and this is the first study utilizing site-directed mutagenesis which suggests a possible role for CPa-1 in water oxidation. In vivo, the substitution of glycines for the basic residue pair ^{384,385}R enhances the rate of photoinactivation, results in the apparent reduction in the number of fully functional PS II centers, and reduces the steady-state oxygen evolution rate by 50%. These results are consistent with the hypothesis that this modification introduces a defect at the oxygen-evolving complex of PS II. In vitro, this site-directed modification results in a marked reduction of water-oxidizing activity and an enhanced ability for DPC to serve as an electron donor to PS II. These results are consistent with this mutation leading to the loss of stability of the oxygen-evolving complex. The precise nature of the lesion introduced within the oxygen-evolving complex is the object of continuing investigations.

ACKNOWLEDGMENT

Special thanks to Ms. Laurie K. Frankel for her help in preparing the manuscript.

REFERENCES

Allen, J. F., & Holmes, N. G. (1986) in *Photosynthesis Energy Transduction* (Hipkins, M. F., & Baker, N. R., Eds.) pp 103–142, IRL Press, Washington, DC.
Amesz, J. (1983) *Biochim. Biophys. Acta 726*, 1–12.
Arnon, D. I. (1949) *Plant Physiol. 24*, 1–15.
Bricker, T. M. (1990) *Photosynth. Res. 24*, 1–13.
Bricker, T. M. (1992) *Biochemistry 31*, 4623–4628.
Bricker, T. M., & Frankel, L. K. (1987) *Arch. Biochem. Biophys. 256*, 295–301.
Bricker, T. M., Odom, W. R., & Queirolo, C. B. (1988) *FEBS Lett. 231*, 111–117.
Burnap, R. L., & Sherman, L. A. (1991) *Biochemistry 30*, 440–446.
Chua, N.-H., & Blomberg, F. (1979) *J. Biol. Chem. 254*, 215–223.
Dismukes, G. C. (1986) *Photochem. Photobiol. 43*, 99–115.
Eaton-Rye, J. J., & Vermaas, W. F. J. (1991a) *Plant Mol. Biol. 17*, 1165–1177.
Eaton-Rye, J. J., & Vermaas, W. F. J. (1991b) *Plant Physiol. s96*, 115.
Enami, I., Satoh, K., & Katoh, S. (1987) *FEBS Lett. 226*, 161–165.
Enami, I., Miyaoka, T., Mochizuki, Y., Shen, J.-R., Satoh, K., & Katoh, S. (1989) *Biochim. Biophys. Acta 973*, 35–40.
Enami, I., Kaneko, M., Kitamura, N., Koike, H., Sinoike, K., Inoue, Y., & Katoh, S. (1991) *Biochim. Biophys. Acta 1060*, 224–232.
Frankel, L. K., & Bricker, T. M. (1989) *FEBS Lett. 257*, 279–282.
Frankel, L. K., & Bricker, T. M. (1990) in *Current Research in Photosynthesis* (Batcheffsky, M., Ed.) Vol. I, pp 825–828, Kluwer Academic Press, Dordrecht.
Frankel, L. K., & Bricker, T. M. (1992) *Biochemistry* (in press).
Ghanotakis, D. F., Demetriou, D. M., & Yocum, C. F. (1987) *Biochim. Biophys. Acta 891*, 15–21.
Hackett, C. S., & Strittmatter, P. (1984) *J. Biol. Chem. 259*, 3275–3282.
Homann, P. H. (1987) *J. Bioenerg. Biomembr. 19*, 105–123.
Ikeuchi, M., Tako, K., & Inoue, Y. (1989) *FEBS Lett. 242*, 263–269.
Kunkel, T. A. (1985) *Proc. Natl. Acad. Sci. U.S.A. 82*, 488–492.
Kuwabara, T., Miyao, M., Murata, T., & Murata, N. (1985) *Biochim. Biophys. Acta 806*, 283–289.
Maniatis, T., Fritsch, E. F., & Sambrook, J. (1982) *Molecular Cloning–A Laboratory Manual*, Cold Spring Harbor Laboratory, Cold Spring Harbor, NY.
Morris, J., & Herrmann, R. G. (1984) *Nucleic Acids Res. 12*, 2837–2850.
Odom, W. R., & Bricker, T. M. (1992) *Biochemistry 31*, 5616–5620.
Philbrick, J. B., Diner, B. A., & Zilinskas, B. A. (1991) *J. Biol. Chem. 266*, 13370–13376.
Rippka, R., Derulles, J., Waterbury, J. B., Herdman, M., & Stanier, R. Y. (1979) *J. Gen. Microbiol. 111*, 1–61.
Tang, X. S., & Satoh, K. (1985) *FEBS Lett. 179*, 60–64.
van der Bolt, F., & Vermaas, W. (1992) *Biochim. Biophys. Acta 1098*, 247–254.
Vermaas, W. F. J., Williams, J. G. K., & Arntzen, C. J. (1987) *Plant Mol. Biol. 8*, 317–326.
Vermaas, W. F. J., Ikeuchi, M., & Inoue, Y. (1988) *Photosynth. Res. 17*, 97–113.
Williams, J. G. K. (1988) *Methods Enzymol. 167*, 766–778.
Yu, J., & Vermaas, W. (1991) *Plant Physiol. s96*, 115.